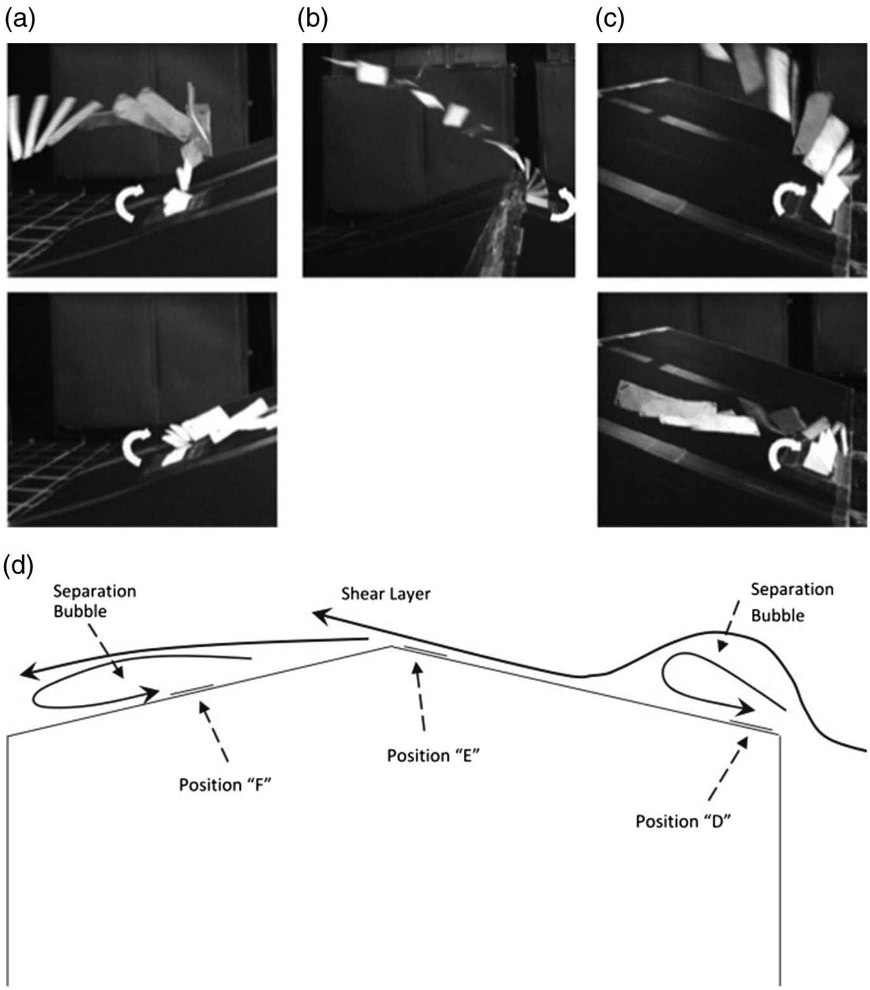

Fig. 4.2. Flight patterns of shingles from a gable roof at three locations: (a) leeward side of the ridge (Position F); (b) windward side of the ridge (Position E); (c) windward eave (Position D); (d) schematic of the flow patterns over the roof for wind from right to left
Source: From Kordi and Kopp (2011)

moment of failure. Of particular importance appear to be the patterns associated with separation "bubbles," where the local flow direction is opposite to the bulk wind direction close to the building surface. When the component can clear the separation bubble, it enters the accelerated flow above the separation bubble and can travel a substantial distance. Components that do not enter this high-speed flow tend to stay on the roof surface. Upstream terrain and surrounding buildings can substantially alter these flow patterns and the subsequent debris trajectories.

4.2.2 Initial Motion—Compact Debris

The initial motion of roof gravel is along the roof surface and is caused by the wind field near the roof surface, i.e., the flow patterns generated by the building. Initially, only a few rocks will be moving, but as the wind speed increases the gravel begins to scour, as shown in Fig. 4.3. This is consistent with the effects of the fixture strength integrity suggested by Wills et al. (2002), where loose-laid objects

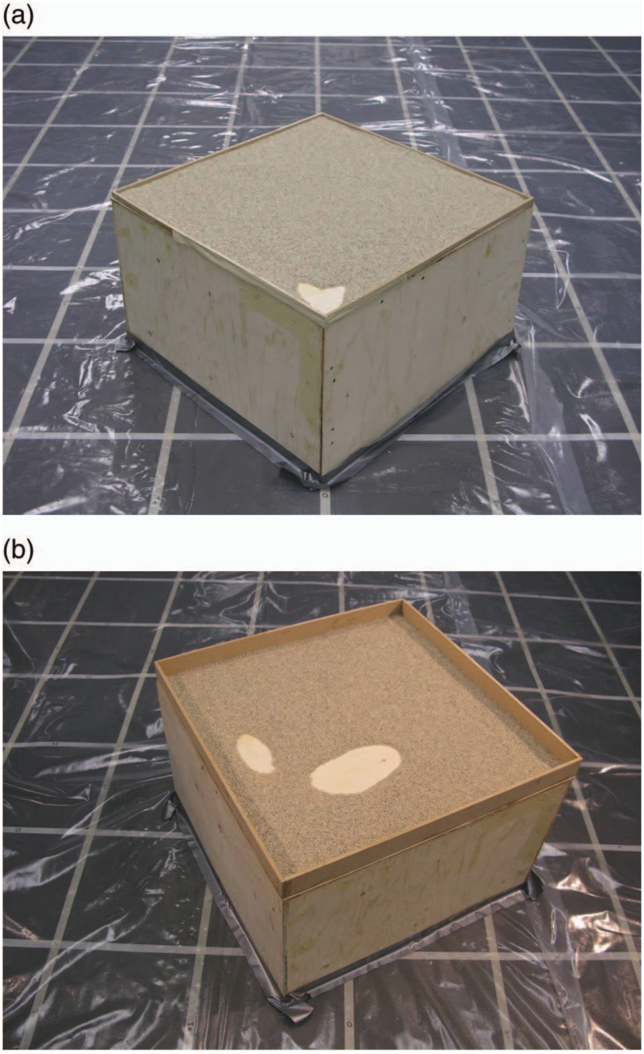

Fig. 4.3. Photograph of gravel scour patterns on the roof of a 7.32 m (24 ft) high building: (a) with a small parapet and a quartering wind (45°), and (b) with a 0.91 m (3 ft) high parapet and a cornering wind (30°) from a 1/20 scale wind tunnel model. The wind direction is approaching from the lower edge in these photographs

tend to move primarily along the surface. Kind (1974a, b) found that the onset speed for a particular building size and shape is proportional to $\sqrt{d}$, where d is the diameter of the gravel. Scour (and flight) speeds also depend on the height of the building, parapet height, surrounding buildings, and wind direction, which alter the wind speeds and patterns near the roof surface. At wind speeds above the scour speed, gravel ballast will leave the roof, typically leaving the roof surface over the windward parapet first, and then, at higher speeds, above the leeward parapet.

Because spherical objects do not tend to generate lift, a vertical component of the wind is required to lift them off the roof surface. Such vertical motions are generated by the flow separations along the roof edges and corners. The so-called corner vortices, discussed in Chapter 3, which are generated by oblique wind directions, induce particularly strong upward motions. Unlike roof components, which are loaded by the pressure fields associated with these vortices, the loads on roof gravel depend on the wind speeds and directions generated by these vortices. One outcome of this is that the dependence on wind direction is particularly significant for gravel motion with the wind speeds required for onset of flight for wind directions normal to the wall being more than double those for quartering winds. In other words, directionality effects are larger for roof gravel than for typical roof components. Quartering winds tend to yield the lowest flight speeds because of the strong vertical flow components associated with cornering vortices. High parapets can substantially increase the onset of flight gust wind speeds, although for typical low-rise buildings, the onset of flight is at wind speeds that are usually below 161 km/h (100 mi/h) for the critical wind directions (Masters and Gurley 2008).

4.2.3 Flight Patterns—Plate-Like Debris

Many of the experiments and analyses on flight of wind-borne debris have focused on uniform, smooth flow with well-defined initial conditions such that the initial forces and moments at release are closely related to the static aerodynamic coefficients. Tachikawa (1983) was the first to do this, but much of the subsequent work has followed this same approach. Such experiments have provided validation for numerical models, debris flight speeds to set impact test criteria (e.g., Lin et al. 2007), and flight trajectories for risk models (e.g., Tachikawa 1988). For plate-like debris, these experiments have shown that the initial conditions have a significant effect on flight trajectories. Depending on the initial angle of attack, ξ, and the Tachikawa number, K, different modes of flight can arise, including cases with (1) significant rotation, (2) mostly translational motion with limited rotation, and (3) reversals of the direction of rotation mid-flight. Fig. 4.4 shows sample trajectories taken from the Tachikawa (1983) seminal work on the two-dimensional motion of plates. These patterns call to mind the patterns of falling paper, the only difference being that falling paper typically is not placed in cross-flow, which is the driving force for wind-borne debris. Visscher and Kopp (2007) have shown these same patterns can arise for debris originating from the roof of a building, with the pattern significantly affecting the total distance the debris flies. Tachikawa (1988) used these significant effects of initial conditions to estimate variability of trajectories in real storms, an approach that has been used many times subsequently, as discussed in

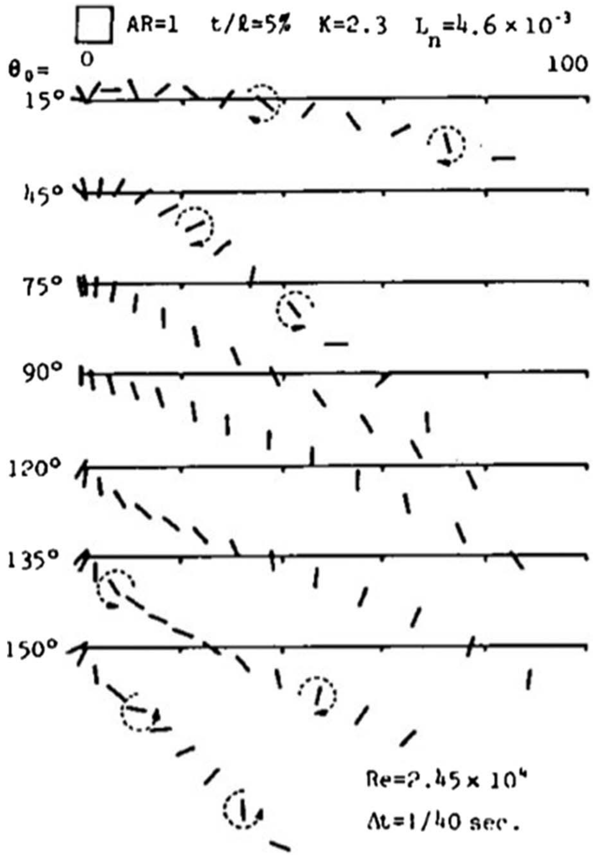

Fig. 4.4. Example of typical trajectories of thin plates in uniform smooth flow for different initial angles of attack
Source: From Tachikawa (1983)

Chapter 6. However, the flow fields near building surfaces and in building wakes, and the source location on the building surface, often play larger roles in determining the actual trajectories (Kordi et al. 2010; Kordi and Kopp 2011).

4.2.4 Overall Flight Distances and Trajectories—Plate-Like Debris

Overall flight distances and trajectories are important for establishing the risk of debris impact. Trajectories depend on the wind speed and direction; the mass and shape of the object; the original location of the component on the source building; the size, shape, and parapet heights of the source building, and the location and height of any adjacent buildings. As shown by Fig. 4.4, there is inherent variability in flight patterns in uniform smooth flow. The variation in the turbulent flow patterns around buildings also causes substantial variation in the subsequent debris trajectory, as indicated by Fig. 4.2. For example, Fig. 4.5 shows the landing locations of shingles originating from different locations on the roof of a house.

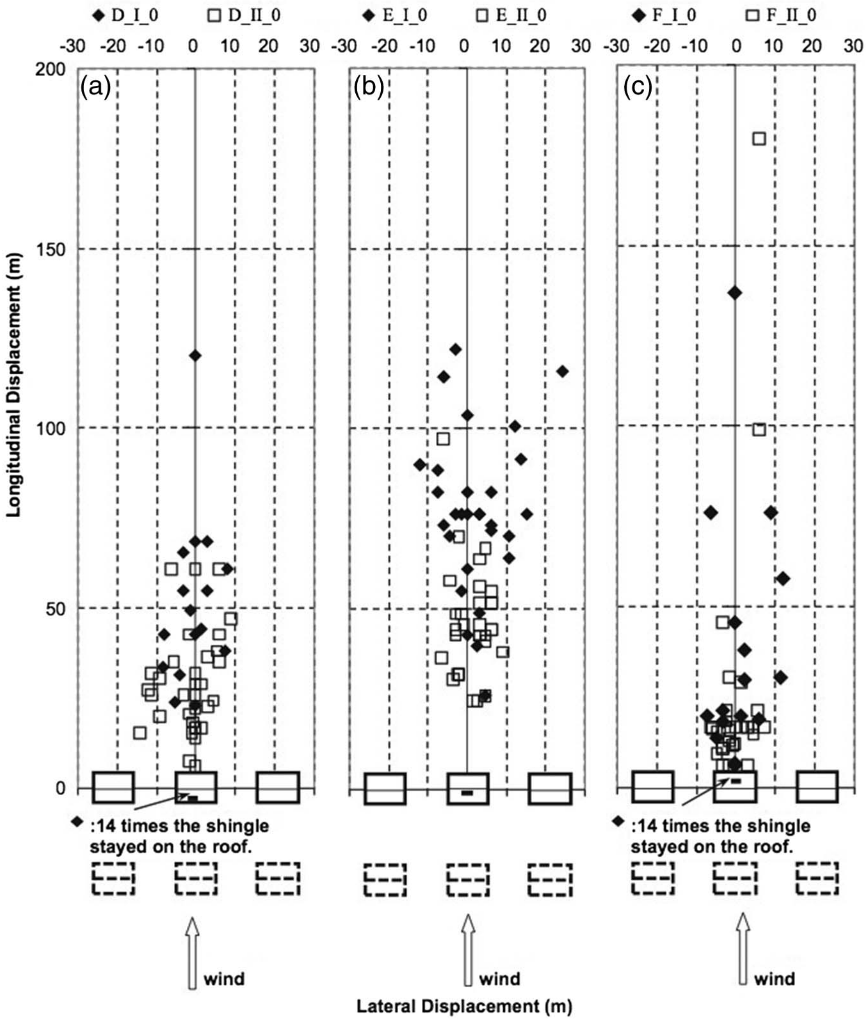

Fig. 4.5. Landing locations for shingles originating from the (a) windward eave, (b) windward side of the ridge, and (c) leeward side of the ridge for a gable-roofed house with (open symbols) and without (closed symbols) surrounding houses
Source: From Kordi and Kopp (2011)

There is clearly a wide variation of landing locations under nominally identical initial conditions, with one source roof position having a range from 0 to ~180 m (0 to ~590 ft) in this particular case. Kordi and Kopp (2011) attributed this primarily to variations in the turbulent velocity field at the location of the shingle at the moment of failure, as well as to variations during flight.

Uniform flow results suggest that the higher the wind speed, the further the flight. However, for debris originating on real buildings, the local flow patterns around the position of the component at the instant of failure play a larger role, altering the flight distances. As a result, numerical solutions to Eq. (4.5) that utilize uniform flow will not always be accurate for modeling flight trajectories because the local variations in wind speed following component failure play a dominant role. Nevertheless, Fig. 4.6 shows that there is a strong correlation between the height the debris obtains during its initial motion and the subsequent distance traveled. Kordi and Kopp (2011) also found that debris reaching higher heights also tends to travel at higher speeds. Numerical models of Eq. (4.5) utilizing uniform, smooth flow, with the uniform wind speed being the 3-s gust speed at the roof height, tend to capture the longest distances such objects can travel, but are unable to capture the variation without additional information.

4.2.5 Overall Flight Distances and Trajectories—Compact Debris

As mentioned, for compact debris it is usual to assume that the lift and moment coefficients are negligible so that the only force coefficient is the drag. Thus, the most common trajectories for gravel are ones where the debris is falling continuously. Trajectories for spheres (gravel) have been examined by Holmes (2004). More recently, Karimpour and Kaye (2012) and Moghim and Caracoglia (2014) examined the effects of turbulence and showed that it substantially increased the variation in the flight distances. Because there is no lift, compact debris requires a vertical wind speed component in order to rise. This occurs in the atmospheric surface layer of hurricanes, although the correlation between the vertical and horizontal wind components is negative, so that upward vertical gusts are usually associated with relatively quiet moments in the horizontal wind while the largest gust speeds are correlated with downward wind components. However, upward wind components occur in the separated flow and vortices caused by roof edges

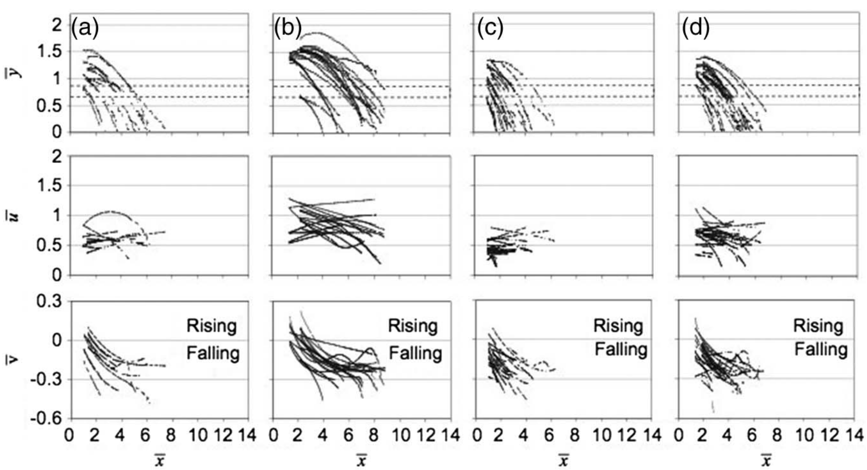

Fig. 4.6. Trajectories and debris speeds for shingles originating from different locations on the roof of a 2-story house
Source: From Kordi and Kopp (2011)

and in the flow field in the vicinity of the upper portions of the windward face of buildings, so the position and relative heights of buildings are important to these trajectories. Post-storm damage surveys have shown that glazing and windows at heights above the source building roof can be broken by gravel (or other broken glass), as discussed in Chapter 2, which is caused by these upward wind components.

4.3 FLIGHT SPEEDS

In uniform, smooth flow, it has been shown (Lin et al. 2007; Letchford et al. 2013) that the debris flight velocity follows the form

$$\overline{u} = 1 - e^{-\sqrt{C_1 K\overline{x}}} \tag{4.15}$$

where $C_1 \sim O(1)$ is a constant that depends on the type and shape of debris object.

Lin et al. (2007) and Letchford et al. (2013) provide values for compact and rod-like debris. For spheres, $C_1 = 1.0$, while for rods $C_1 = 1.6$ (Letchford et al. 2013). These curves show that the non-dimensional distance to the asymptotically limited wind speed is roughly $K\overline{x} \sim 4$ if $C_1 = 2$ and $K\overline{x} \sim 9$ if $C_1 = 1$.

For a rock of diameter 16 mm (0.63 in.) and weight of 5.4 g, $\overline{u} = 1 - e^{-\sqrt{0.022x}}$. For example, for a 7.3 m (24 ft) tall building and a basic wind speed [i.e., 3-s gust at 10 m (32.8 ft) in open terrain] of 193 km/h (120 mi/h), gravel may be expected to travel at least 20 m (65.6 ft). In this case, $\overline{u} = 0.48$, so that the dimensional horizontal speed would be 87 km/h (54 mi/h). Of course, one may expect substantial variation in the trajectory distance so that if it traveled 50 m (164 ft), the resulting speed would be 118 km/h (73 mi/h).

For a 2.4 m (8 ft) long 2 × 4 lumber with a weight of 4.1 kg (9 lb), the non-dimensional debris speed would be $\overline{u} = 1 - e^{-\sqrt{0.058x}}$. Fig. 4.7 depicts the solution to this equation as a function of horizontal displacement, indicating that 2 × 4 lumber traveling 20 m (65.6 ft) will have a speed of about 65% of the roof height gust speed, while at 40 m (131 ft) it will travel at about 80% of the gust speed. Of course, it must be emphasized that there would be a great deal of scatter in the landing locations, but flight distances of 20–40 m (65.6–131 ft) from 2-story houses would be expected (noting that there are no published studies considering these distances with sources from real buildings, possibly due to the extreme complexity in the initial conditions). The asymptotic limit of the speed for a 2 × 4 lumber is reached at $K\overline{x} \sim 5$, which translates to $x \sim 140$ m (459 ft). These speeds can be compared with standardized impact test requirements, as discussed in Chapter 7.

For plates, the form of Eq. (4.15) is not consistent with the asymptotic limits in Eq. (4.11). The data in Fig. 4.6 also show that the form $\overline{u} = f(x)$ as indicated by Eq. (4.15) does not tend to occur in debris flights originating from roofs of buildings. For plate debris with higher values of K (i.e., lighter elements), such as plywood or oriented strand board roof sheathing panels or asphalt shingles, the

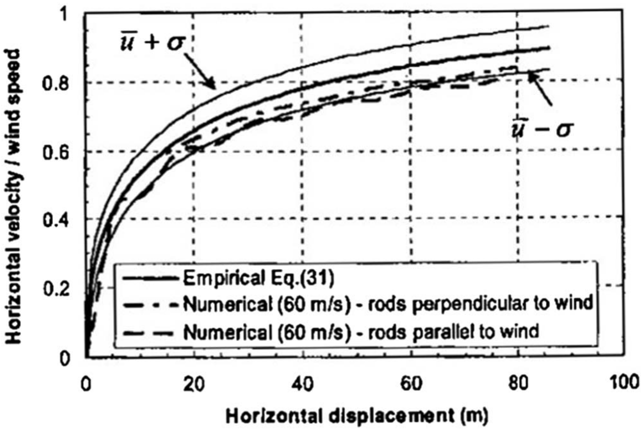

Fig. 4.7. Horizontal speed of a 2.4 m (8 ft) long, 4.1 kg (9 lbs) 2 × 4 lumber as a function of horizontal displacement for a gust speed of 214 km/h (133 mi/h)
Source: From Lin et al. (2007)

asymptotic limit provides a good estimate of the upper bound of the flight speed, using the 3-s gust speed at roof height. The range of speeds for plywood sheathing originating from a 2-story house is typically in the range of 20–90% of the 3-s gust speed at roof height (Kordi et al. 2010), while for shingles the range is 40–120% (Kordi and Kopp 2011). For roof tiles, which are much heavier, the non-dimensional flight distances are much shorter, typically, less than $K\overline{x} \sim 1$ (Kordi and Kopp 2011) for a 7.3 m (24 ft) high source building (e.g., a 2-story house). As a result, flight speeds are lower, typically, in the range of 30–60% of the 3-s gust speed at roof height, which is substantially lower than the asymptotic limit.

References

ASCE. (2010). "Minimum design loads for buildings and other structures." *ASCE/SEI 7-10*, Reston, VA.

Baker, C. J. (2007). "The debris flight equations." *J. Wind Eng. Ind. Aerodyn.*, **95**(5), 329–353.

Holmes, J. D. (2004). "Trajectories of spheres in strong winds with application to wind-borne debris." *J. Wind Eng. Ind. Aerodyn.*, **92**(1), 9–22.

Holmes, J. D., Baker, C. J., and Tamura, Y. (2006). "Tachikawa number: A proposal." *J. Wind Eng. Ind. Aerodyn.*, **94**(1), 41–47.

Karimpour, A., and Kaye, N. (2012). "On the stochastic nature of compact debris flight." *J. Wind Eng. Ind. Aerodyn.*, **100**(1), 77–90.

Kind, R. J. (1974a). "Estimation of critical wind speeds for scouring of gravel or crushed stone on rooftops." *LTR-LA-142*, National Research Council of Canada, Ottawa, Canada.

Kind, R. J. (1974b). "Wind tunnel tests on some building models to measure wind speeds at which is gravel is blown off rooftops." *LTR- LA-146*, National Research Council of Canada, Ottawa, Canada.

Kordi, B., and Kopp, G. A. (2009). "Evaluation of the quasi-steady theory applied to windborne flat plates in uniform flow." *J. Eng. Mech.*, **135**(7), 657–668.

Kordi, B., and Kopp, G. A. (2011). "Effects of initial conditions on the flight of windborne plate debris." *J. Wind Eng. Ind. Aerodyn.*, **99**(5), 601–614.

Kordi, B., Traczuk, G., and Kopp, G. A. (2010). "Effects of wind direction on the flight trajectories of roof sheathing panels under high winds." *Wind Struct.*, **13**(2), 145–167.

Letchford, C., Lin, N., and Holmes, J. (2013). "Windborne debris in horizontal winds and applications to impact testing." Chapter 8, *Advanced structural wind engineering*, Y. Tamura and A. Kareem, eds., Springer, Tokyo, 197–215.

Lin, N., Holmes, J. D., and Letchford, C. W. (2007). "Trajectories of wind-borne debris in horizontal winds and applications to impact testing." *J. Struct. Eng.*, **133**(2), 274–282.

Lin, N., Letchford, C., and Holmes, J. D. (2006). "Investigation of plate-type windborne debris. Part I. Experiments in wind tunnel and full scale." *J. Wind Eng. Ind. Aerodyn.*, **94**(2), 51–76.

Masters, F., and Gurley, K. (2008). "Performance of embedded gravel roof systems in extreme wind loading." Univ. of Florida, Gainesville, FL.

Moghim, F., and Caracoglia, L. (2014). "Effect of computer-generated turbulent wind field on trajectory of compact debris: A probabilistic analysis approach." *Eng. Struct.*, **59**, 195–209.

Tachikawa, M. (1983). "Trajectories of flat plates in uniform flow with application to wind-generated missiles." *J. Wind Eng. Ind. Aerodyn.*, **14**(1–3), 443–453.

Tachikawa, M. (1988). "A method for estimating the distribution range of trajectories of wind-borne missiles." *J. Wind Eng. Ind. Aerodyn.*, **29**(1–3), 175–184.

Visscher, B. T., and Kopp, G. A. (2007). "Trajectories of roof sheathing panels under high winds." *J. Wind Eng. Ind. Aerodyn.*, **95**(8), 697–713.

Wills, J. A. B., Lee, B. E., and Wyatt, T. A. (2002). "A model of wind-borne debris damage." *J. Wind Eng. Ind. Aerodyn.*, **90**(4–5), 555–565.

CHAPTER 5

Damage from Impact (Experimental and Theoretical)

David Henderson*
Daniel Smith*
Russell Carter†
Douglas Smith†

Impact from wind-borne debris and the consequences of a breach in the building envelope during windstorms are design load criteria that need to be considered in addition to other design actions such as the wind pressure and dynamic load cycles. Debris mainly impacts windward walls (including doors and windows) and the upwind slope of roofs (Fig. 5.1), as discussed in Chapter 2. Damage investigations have shown that building envelopes constructed from light-weight cladding, glass windows, and roof tiles are especially susceptible to debris impact damage. Such damage can create openings in the building envelope, resulting in large internal pressures and an increased probability of more serious damage to the structure due to pressurization or water ingress.

5.1 INTRODUCTION

Observations after past windstorm events have shown impact damage to buildings caused by structural members such as timber (Fig. 5.2) or steel rafters, battens, and studs, and also by sections of roof that dislodged from adjacent buildings (Fig. 5.3). Often, a domino effect was evident, where debris from a building impacts another building downwind, which in turn increases internal pressure, causing the structure to fail and generate more debris that becomes available to impact other

*Cyclone Testing Station, James Cook University, Townsville, QLD, Australia.

†Department of Civil, Environmental, and Construction Engineering, Texas Tech University, Lubbock, TX, USA.